Chapter 4

The Synthesis of Self-Assembling Dendrimers

4.1. Introduction

While dendrimers are beginning to find their potential applications in the fields of molecular electronics,[1,2] material science (high performance polymers, catalysts, adhesives etc.),[3-6] and membrane chemistry,[7-10] structural control[11] and synthetic efficiency still remain the major issues in dendrimer research. Three synthetic methods (convergent,[12] divergent,[13,14] and double-stage convergent[15]) are recognized, up to now, for high molecular weight, monodisperse dendrimer synthesis. Recently, Zimmerman introduced a self-organizing synthetic approach, which guarantees structural accuracy while eliminating steps from the conventional multistep approach.[16,17] In this case, six subunits were brought together by hydrogen bonding to construct supramolecular dendritic structures up to the fourth generation. In this chapter we describe a concise self-organizing dendrimer synthesis in which 1:3 pseudorotaxane complexes between a triply charged ammonium salt (**1**)[18] (Figure 4.1) and substituted dibenzo-24-crown-8 (DB24C8) units make up the core portions of the dendritic architectures. This is based on the finding of Stoddart et al. that DB24C8 forms pseudorotaxanes with dibenzylammonium salt **2** through noncovalent bonding.[19,20]

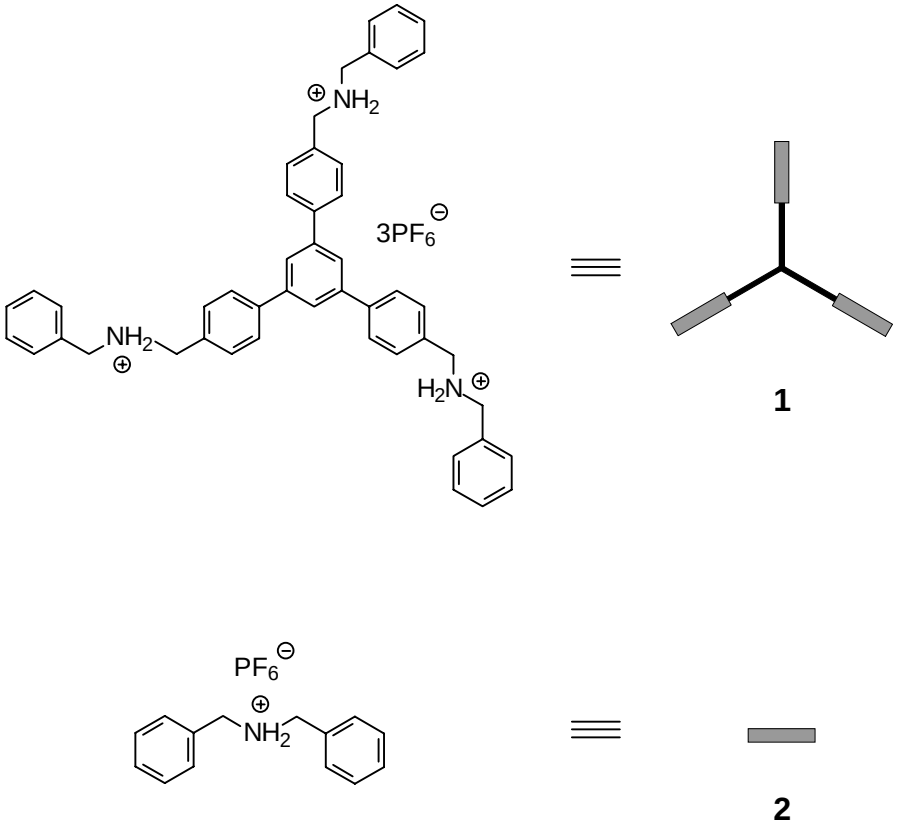

Figure 4.1. Cartoon representations of triply charged ammonium salt **1** and dibenzyl ammonium hexafluorophosphate **2**.

4.2. Results and Discussion

4.2.1. Synthesis

The cyclization reaction between tri(ethylene glycol)dichloride and methyl 3,4-dihydoxybenzoate in a high dilution condition gave 4-carbomethoxydibenzo-24-crown-8 in 40% yield. In order to attach various generations of dendrons to DB24C8, the ester functionality was converted to a carboxylic acid, which was later halogenated to enhance the reactivity toward primary alcohols. The reaction involving the acid chloride functionalized DB24C8 and the 1st generation dendron bearing a primary alcohol ([G1]-OH) gave a poor yield of the desired product. The acid sensitive nature of [G1]-OH gives rise to a great possibility of acid catalyzed side reactions, although the reaction was carried out in the presence of pyridine. HCl generated presumably activated [G1]-OH by protonating the phenolic oxygens, cleaving the benzyl units off. This is evidenced by the ^{1}H NMR spectrum of the crude products. Despite the difficulties encountered in the

purification stage, the product, DB24C8[G1], was isolated as a white solid in 17% yield. The ^{1}H NMR spectrum of DB24C8[G1] shows two sharp singlets at 5.03 and 5.25 ppm for two types of benzylic protons of the dendron unit, G1, integrating for four and two protons, respectively. The signals for the ethyleneoxy units of the crown ether unit appear in the region between 3.81 and 4.19 ppm. Because the reactions described above were not successful in terms of giving acceptable yields, an alternative route was sought.

In the alternative approach, the ester group of 4-carbomethoxydibenzo-24-crown-8 was hydrolyzed and then esterified with a series of benzyl ether dendrons bearing primary alcohol moieties ([G1]-OH, [G2]-OH and [G3]-OH)[12] using the redox system diethyl azodicarboxylate (DEAD) and triphenylphosphine (TPP)[21,22] to afford the corresponding dendrons with the macrocyclic unit at the focal points (**3**, **4**, and **5**) in excellent yields (Figure 4.2).

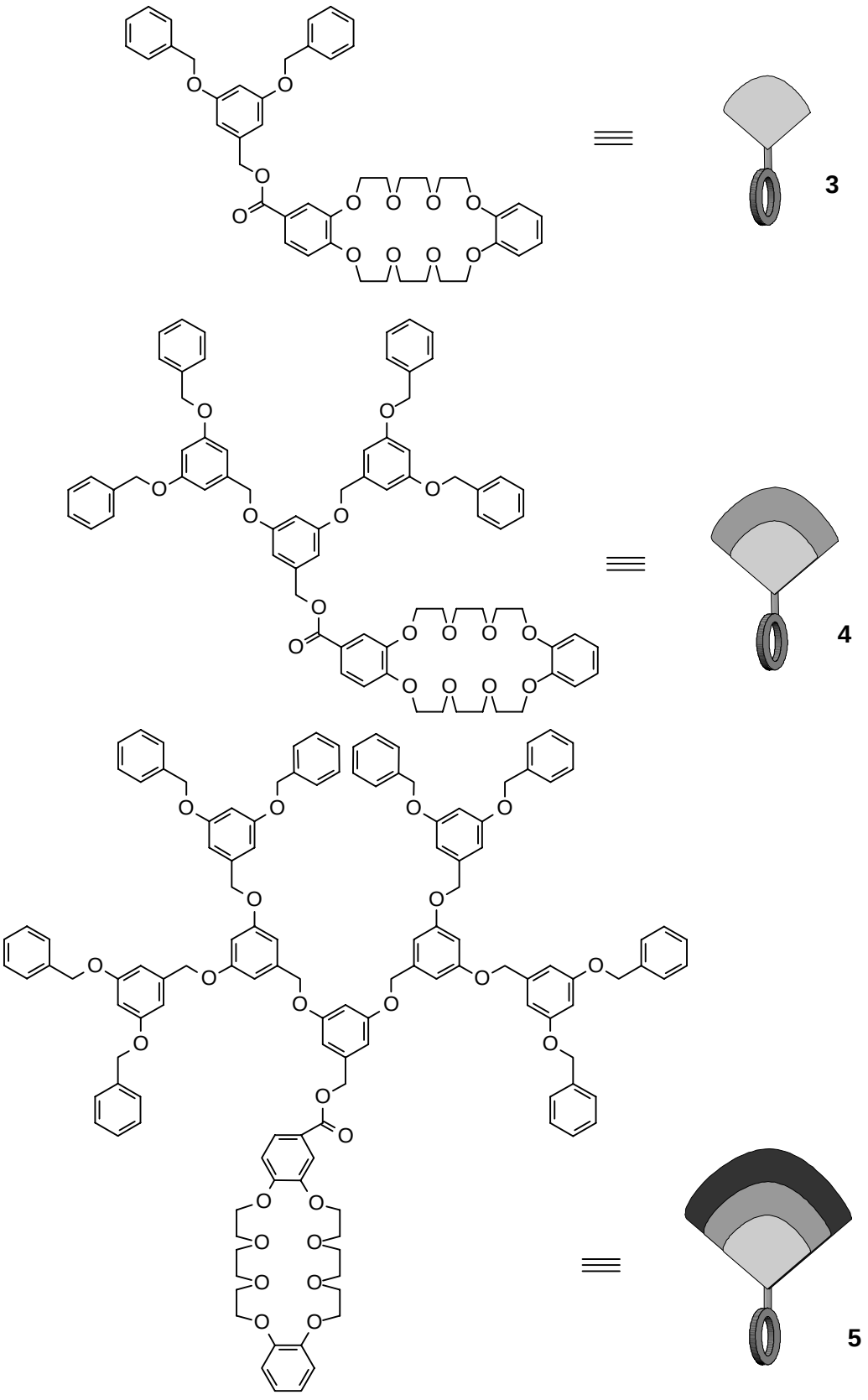

Figure 4.2. Cartoon representations of **3**, **4**, and **5**.

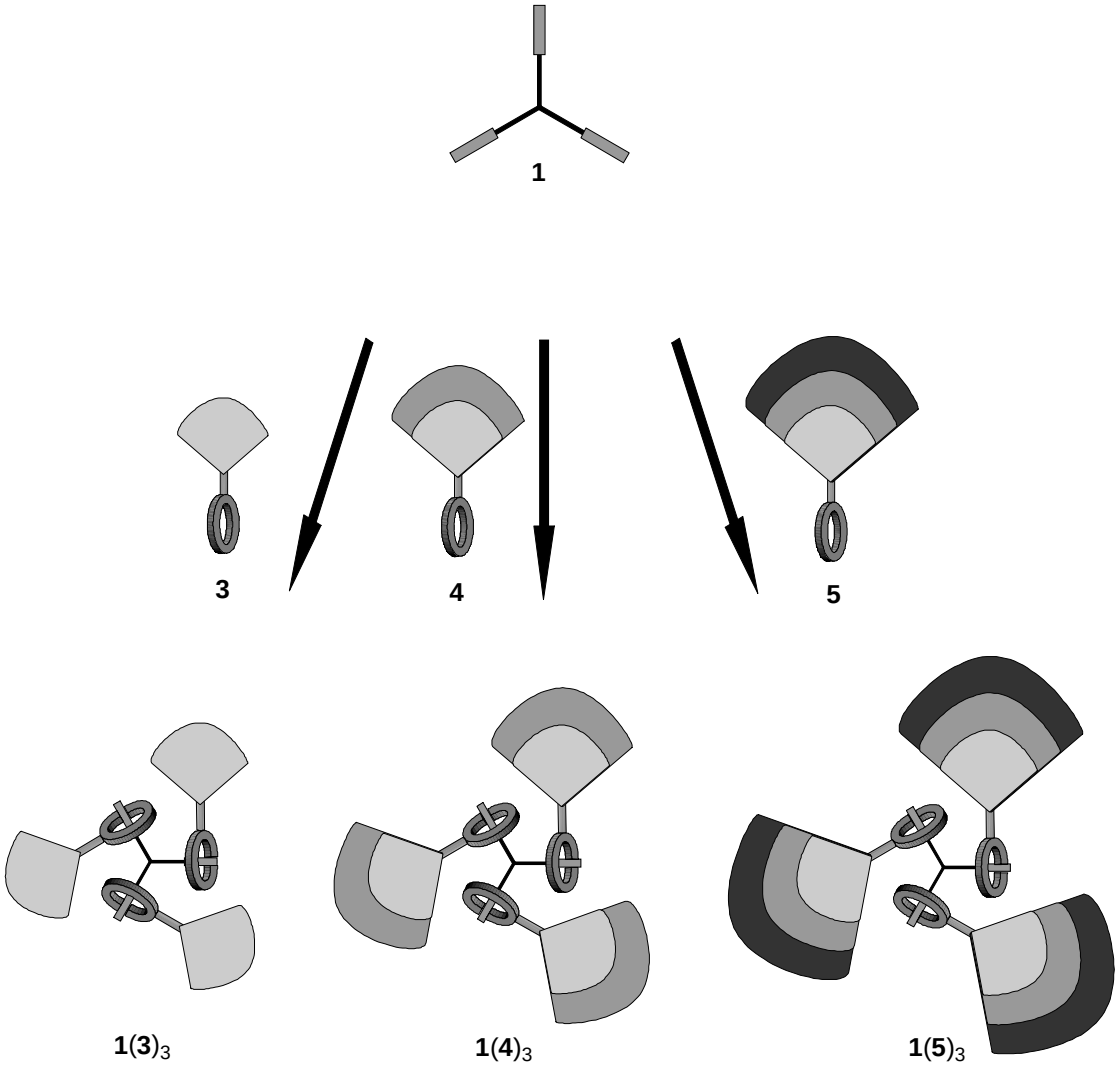

Figure 4.3. Illustrations of the construction of a series of self-assembling dendritic pseudorotaxanes from complementary building blocks.

4.2.2. Complexation studies in chloroform

Our strategy to construct a series of self-organizing dendrimers is illustrated in Figure 4.3. Figure 4.4 shows the aliphatic region of stacked ^{1}H NMR spectra of **1** and **3** as a function of time. The designation of the benzylic protons in **1** and 1st generation dendron **3** for the ^{1}H NMR signal assignments are given in Figure 4.5. 10 min after mixing Figure 4.4b barely reveals new signals corresponding to the complexed species. However, 15 h after mixing, Figure 4.4c clearly shows the newly emerging signals for complexed guest **1** and complexed host **3**. The signals at 4.57 and 4.68 ppm correspond to H_e and H_d protons, respectively, of the complexed ammonium salt guest moiety. It

should be noted that **1** is insoluble in chloroform-*d*. Characteristic chemical shifts for the crown ether host moiety of complexed **3** are detected in the region of 3.55-4.30 ppm.

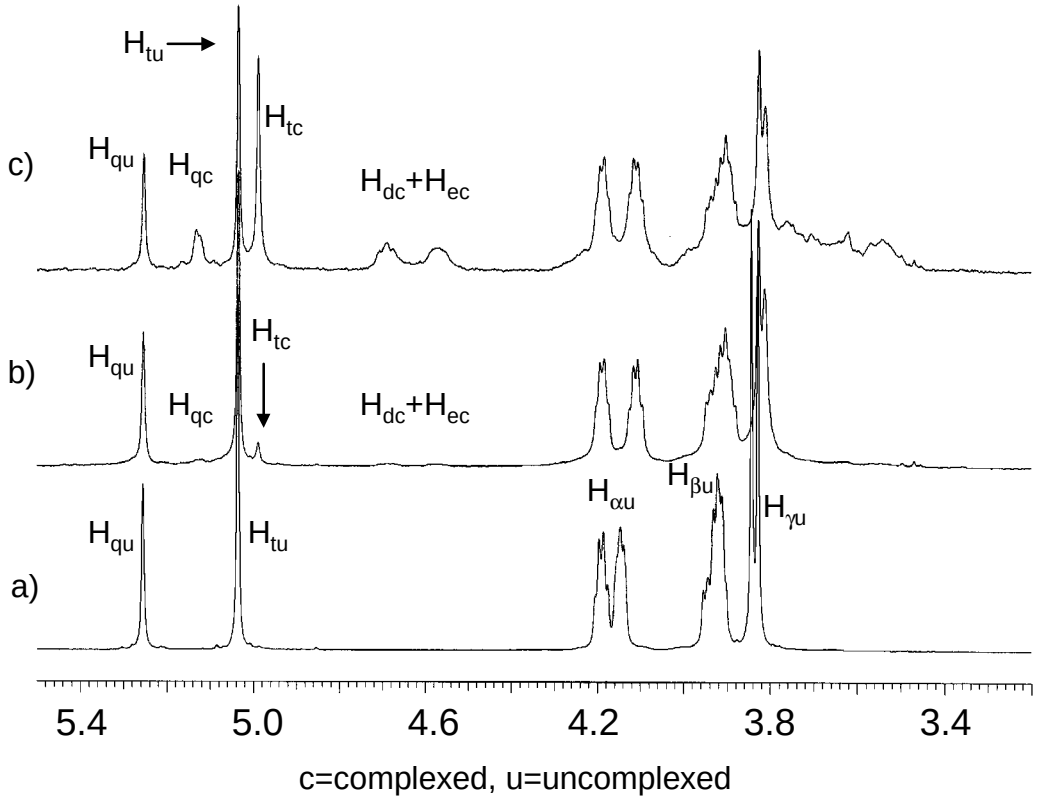

Figure 4.4. The aliphatic region of stacked ^{1}H NMR spectra of a) a 3.0 x10^{-2} M solution of 1st generation dendron **3** and a 3.0 x10^{-2} M solution of **3** mixed with 1/3 mol equivalent of solid **1** after b) 10 min and c) 15 h (400 MHz, chloroform-*d*, 22^{o}C).

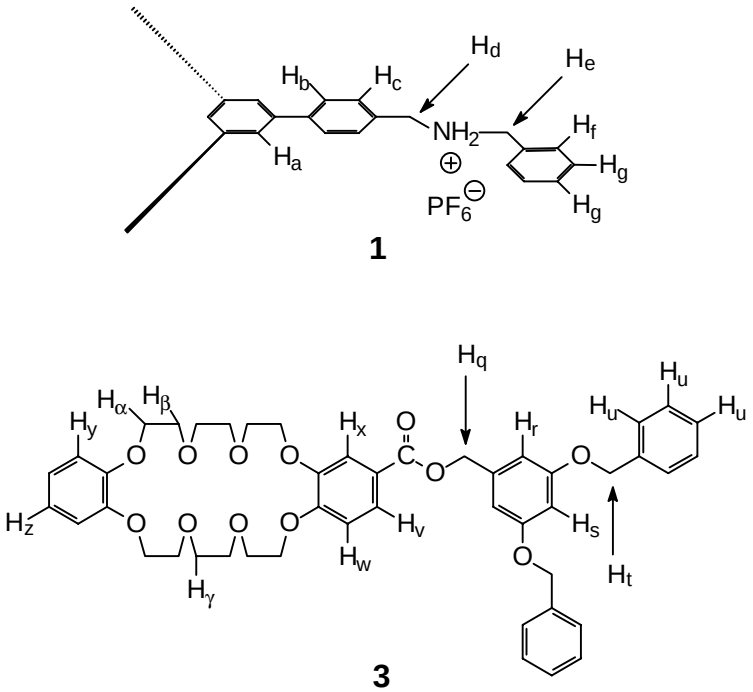

Figure 4.5. The designation of the benzylic protons in **1** and **3** for the signal assignments.

The first evidence of the wholly complexed 1st generation dendrimer **1**(**3**)$_3$ came from the integration study on the ^{1}H NMR spectra in Figures 4.4c. As shown in Figure 4.5, the signals for H_d, H_e, H_q, and H_t protons in the 1:3 complex should integrate in the ratio of 2:2:2:4. Indeed, the signals at 4.68, 4.57, 4.99, and 5.12 ppm (H_d, H_e, H_q, and H_t, protons, respectively, for complexed **3**) integrated for the ratio 2.00, 2.29, 2.06, and 3.80, respectively. The signal assignment on the ^{1}H NMR spectra in the aromatic region (Figure 4.6) was achieved with 2D NMR spectroscopy. In Figure 4.6c the signals of H_a, H_c and H_b protons of complexed **1** appear at 7.82, 7.78 and 7.60 ppm, respectively, after 15 h of mixing. A doublet at 7.51 ppm corresponds to H_b of complexed **1**. The sharp singlet observed for H_a and well-resolved doublets for H_b and H_c indicate that these protons are in magnetically equivalent environments, confirming the sole existence of the 1:3 complex but not 1:2 or 1:1 complexes.

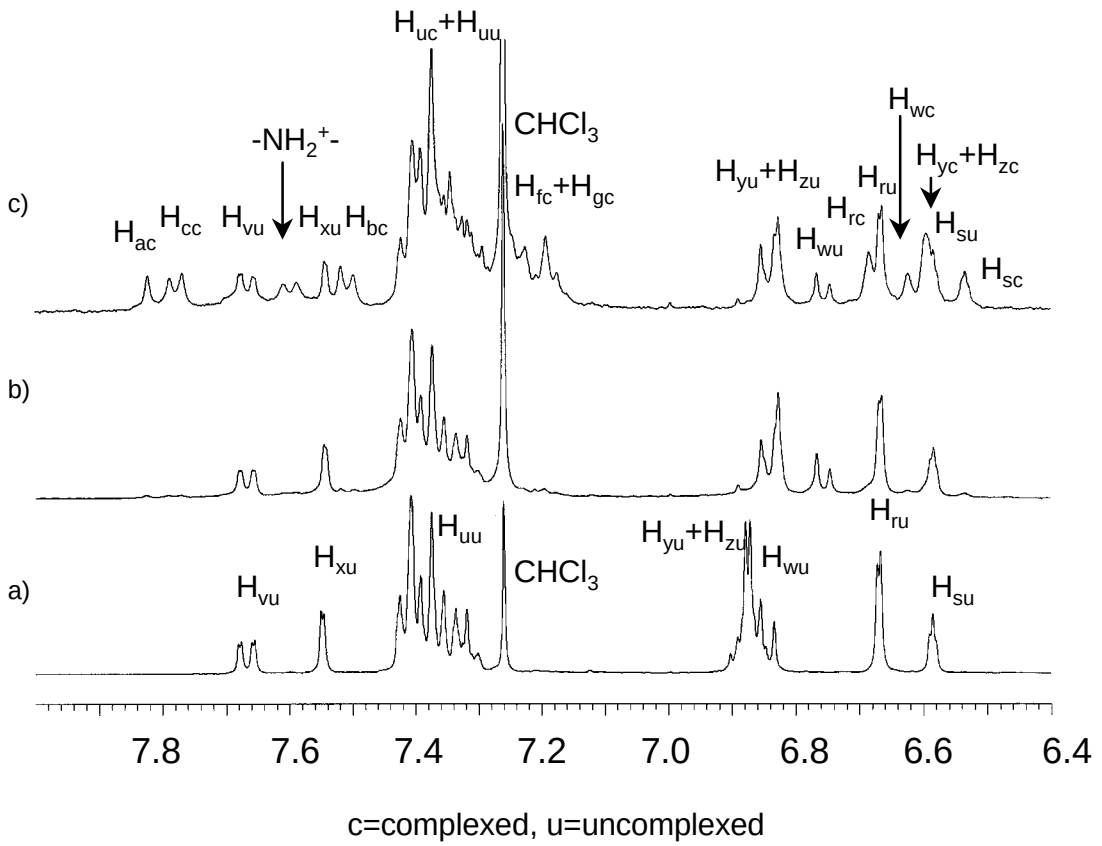

Figure 4.6. The aromatic region of stacked ^{1}H NMR spectra of a) a 3.0 x10^{-2} M solution of **3** and a 3.0 x10^{-2} M solution of **3** mixed with 1/3 mol equivalent of solid **1** after b) 10 min and c) 15 h (400 MHz, chloroform-*d*, 22^{o}C).

The ^{1}H NMR spectra were recorded 10 min, 2 h, 2 days, and 7 days after mixing a 3.0 x 10^{-2} M chloroform solution of 2nd generation dendron **4** with solid **1**. Similar to the spectroscopic data obtained for the 1st generation self-assembling dendrimer, the complexation process was clearly noticed by the newly emerging signals corresponding to the benzylic protons of complexed host **4**. The signals for H_d and H_e protons of complexed **1** were also detected, indicating that **1** became soluble upon the formation of the 2nd generation dendrimer.

In the case of the 3rd generation dendritic pseudorotaxane, when a 3.0 x 10^{-2} M solution of 3rd generation dendron **5** in chloroform-*d* was mixed with 1/3 molar equivalent of solid **1**, the ^{1}H NMR spectrum of the mixture revealed signals associated with the complexed ammonium salt moiety of **1**, complexed **5**, and uncomplexed **5** on the basis of slow association and dissociation on the ^{1}H NMR time scale (Figure 4.7). A

gradual dissolution of otherwise insoluble **1** with increasing mixing time was evidenced by the appearance of the new signals for the complexed ammonium salt moiety of **1**, H_{dc} and H_{ec} (see Figure 4.8), and their gradual increase in intensity. The stoichiometry of the complex was determined to be 1:3 by simple integration of the signals for relevant protons since the signals for the uncomplexed ammonium salt moiety of **1**, H_{du} and H_{eu}, were undetected, indicating the absence of the 1:1 and 1:2 complexes in the chloroform solution. The sole existence of the wholly complexed dendrimer was also demonstrated in the aromatic region of the ^{1}H NMR spectrum (Figure 4.9), which showed that the signal for H_{ac} proton was a singlet and the signals for H_{ac}, H_{kc}, and H_{dc}+H_{ec} protons were integrated to be 1:2:4 in ratios. A total of 17, 57, and 59% of **1** were taken into solution after 10 min., 48 h, and 72 h, respectively, and the complexation process finally reached equilibrium after 72 h.

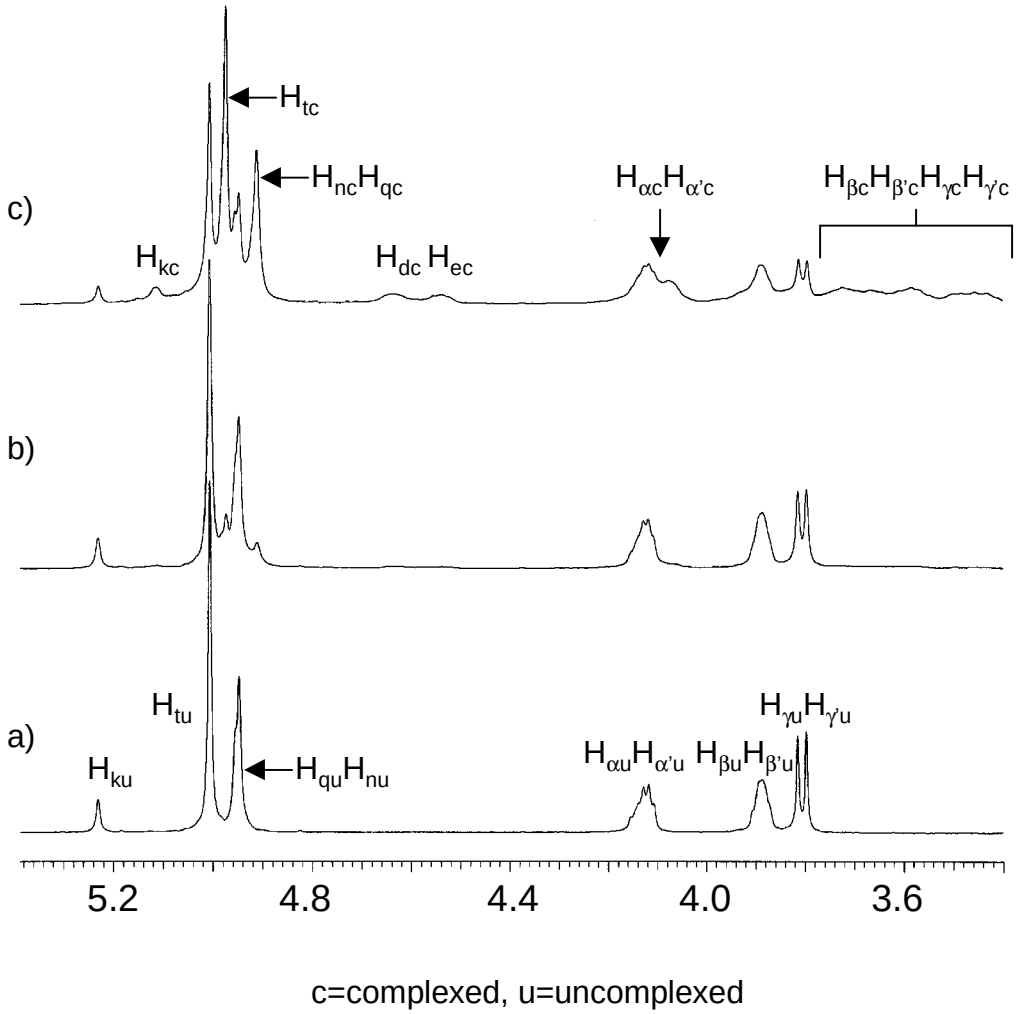

Figure 4.7. The aliphatic region of stacked ^{1}H NMR spectra of a) a 3.0 x 10^{-2} M solution of 3rd generation dendron **5** and a 3.0 x 10^{-2} M solution of **5** mixed with 1/3 molar equivalent of solid **1** recorded after b) 10 min., and c) 72 h (400 MHz, chloroform-*d*, 22^{o}C).

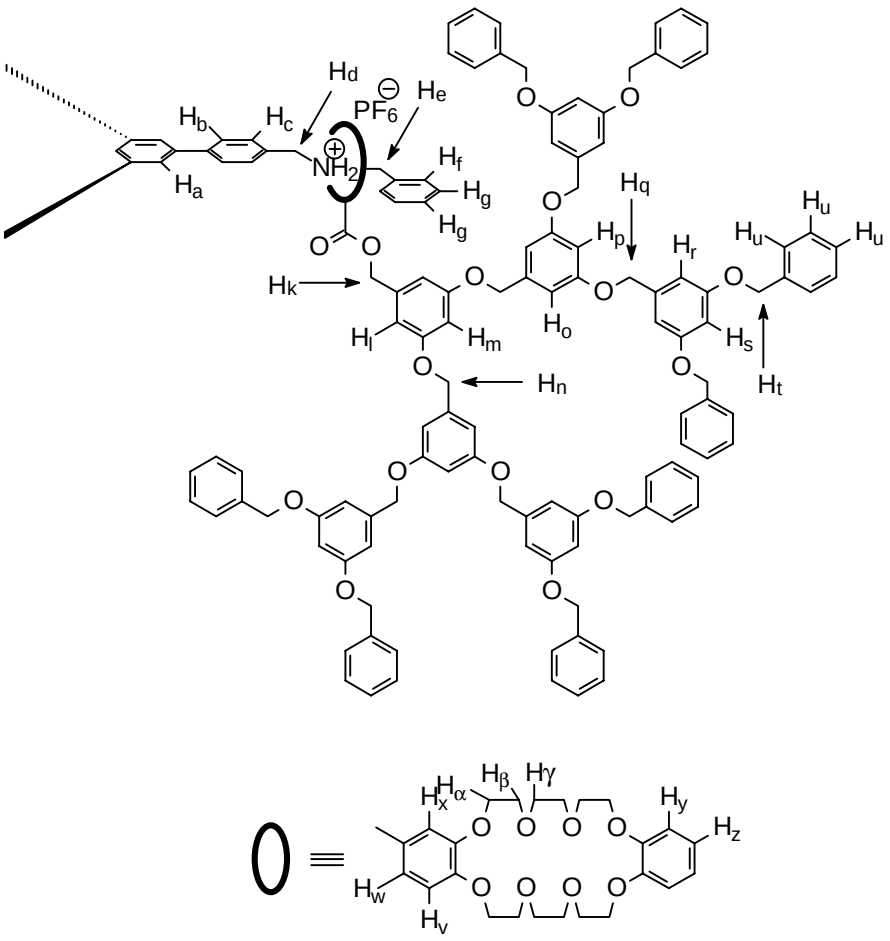

Figure 4.8. The designation of the benzylic protons in **1** and **5** for the signal assignments.

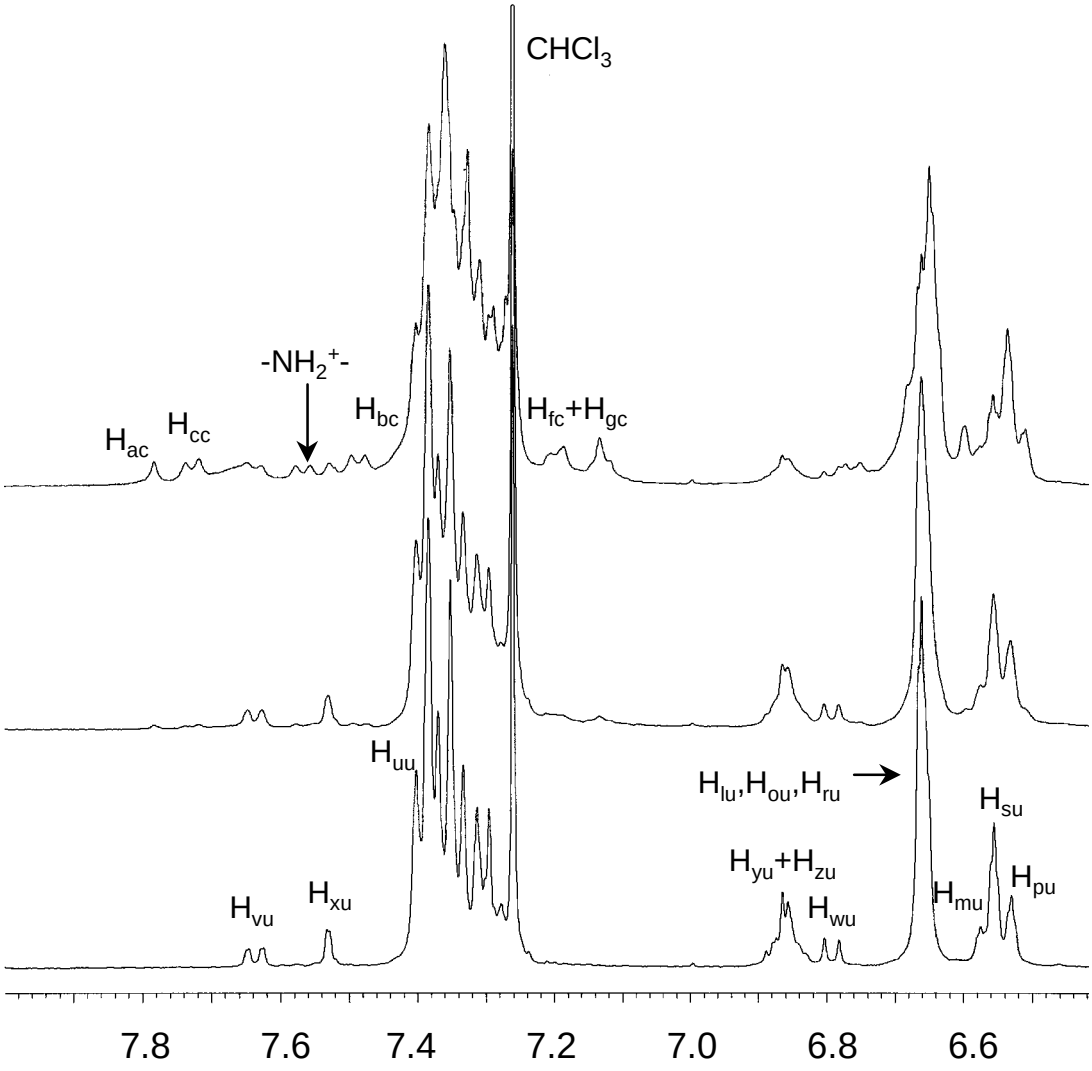

Figure 4.9. The aromatic region of stacked ^{1}H NMR spectra of a) a 3.0 x 10^{-2} M solution of **5** and a 3.0 x 10^{-2} M solution of 3rd generation dendron **5** mixed with 1/3 molar equivalent of solid **1** recorded after b) 10 min., and c) 72 h (400 MHz, chloroform-*d*, 22^{o}C).

The slow formation of dendritic pseudorotaxane **1**(**5**)$_3$ is presumably due to a combination of the poor solubility of **1** and steric hindrance experienced by neighboring dendron units in the 1:3 complex. The latter can be explained by the following two spectroscopic observations. 1) Significant upfield chemical shifts were observed for the complexed benzylic protons of **5** in **1**(**5**)$_3$, H_{kc}, H_{nc}, H_{qc}, and H_{tc} (see Figure 4.8), in Figure

4.7. In contrast, the ^{1}H NMR spectra of a 1.0 x 10^{-2} M solution of **5** in chloroform-*d* mixed with 1 molar equivalent of solid dibenzylammonium hexafluorophosphate (**2**) recorded periodically with increasing mixing time were identical and showed that the signals for the benzylic protons of dendron **5** in the 1:1 complex **2**(**5**) were not distinguishable from those of uncomplexed **5**. 2) Similar ^{1}H NMR experiments to construct the dendritic pseudorotaxanes **1**(**3**)$_3$ and **1**(**4**)$_3$ in chloroform-*d* revealed that the complexation processes equilibrated faster with decreased bulkiness of the dendron units (after 36 and 48 h, respectively).

4.2.3. Complexation studies in acetone

As observed with model system of **1** and DB24C8 in chapter 3, in the ^{1}H NMR spectra of acetone solutions of **1** and 1st generation dendron **3** the signals for uncomplexed benzylic protons of **1** (H_{du} and H_{eu}) shifted significantly upfield (Figure 4.10). The signals for H_{du} and H_{eu} originally resonated as two sharp singlets at 5.26 and 5.11 ppm, respectively, but gradually shifted upfield and changed their shapes to give multiple peaks while they decreased their intensity as the concentration of **3** was increased. Since the signals for H_{du} and H_{eu} are starting to overlap with the signals for $H_{\alpha c}$ at 0.01M/0.03M (**1**/**3**), the monitoring of the signals (H_{du} and H_{eu}) in terms of chemical shifts, signal pattern changes, and peak intensity becomes an uneasy task above this concentration. The signals for the benzylic protons of the dendron unit, H_{qu} and H_{tu}, also give distinguishable upfield chemical shifts upon complexation (Figure 4.10). The nature of the signal patterns and the precise chemical shifts of H_{qc} and H_{tc} are not understood fully at this point because the signals for H_{qc} and H_{tc} cannot be completely differentiated from H_{qu} and H_{tu}.

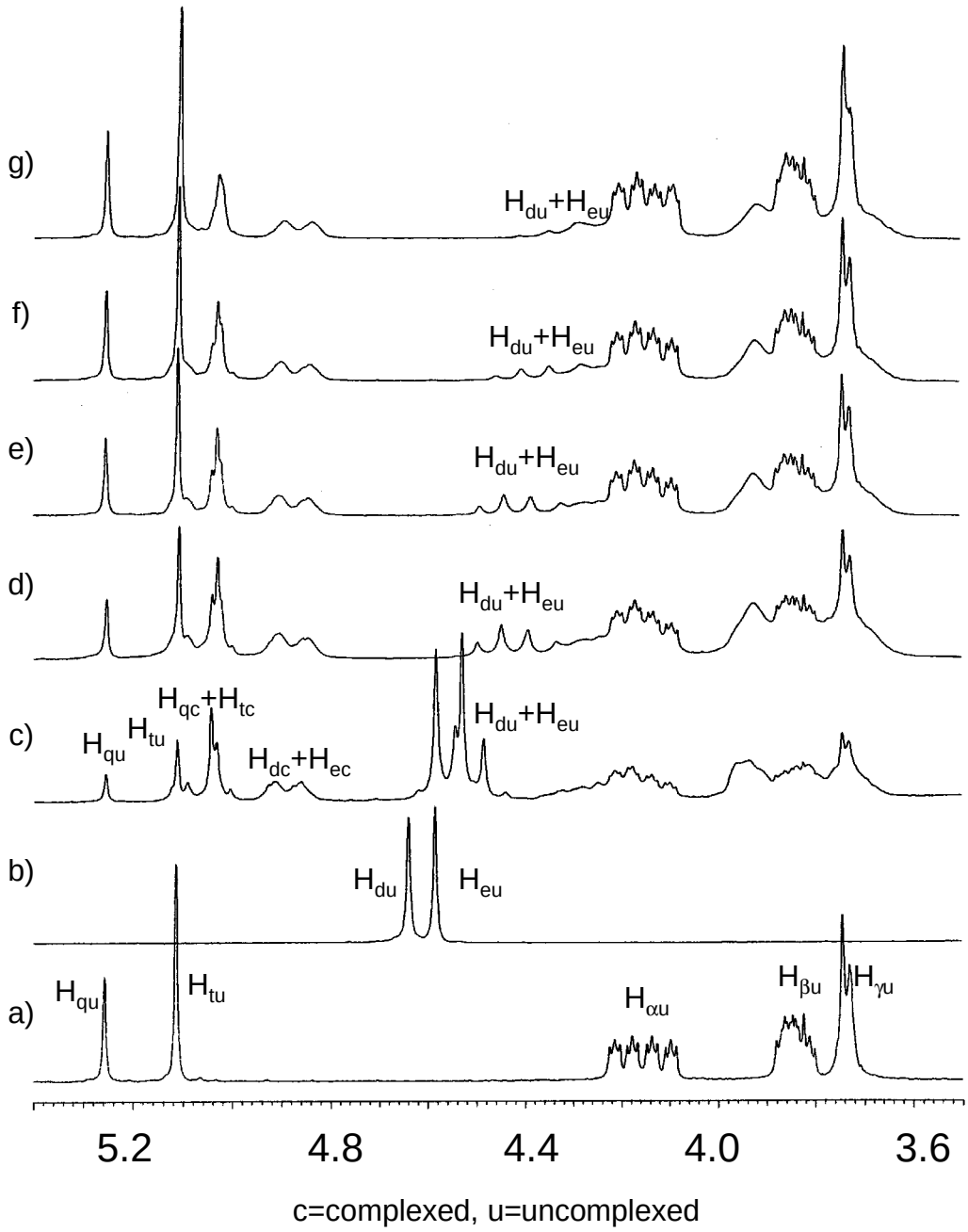

Figure 4.10. The aliphatic region of stacked ^{1}H NMR spectra of solutions of **1** and 1st generation dendron **3** at a) 0/1.0 x 10^{-2}, b) 1.0 x 10^{-2}/0, c) 1.0 x 10^{-2}/1.0 x 10^{-2}, d) 1.0 x 10^{-2}/3.0 x 10^{-2}, e) 1.0 x 10^{-2}/4.0 x 10^{-2}, f) 1.0 x 10^{-2}/5.0 x 10^{-2}, and g) 1.0 x 10^{-2} M/6.0 x 10^{-2} M (400 MHz, acetone-d_6, 22^{o}C).

The aliphatic region of stacked ^{1}H NMR spectra of solutions of **1** and 2nd generation dendron **4** exhibit four different sets of signals corresponding to complexed **1**, complexed **4**, free **1**, and free **4** in acetone-d_6 (Figure 4.11), suggesting a slow exchange

of the two recognition sites on the ^{1}H NMR time scale. The signals for complexed H_α, H_β, and H_γ protons resonate in the region of 3.48-4.34 ppm as small but observable peaks underneath the signals for uncomplexed H_α, H_β, and H_γ protons. Most intriguing chemical shifts and splitting pattern changes were observed for H_{du} and H_{eu} as the concentration of **4** was increased. As predicted based on our preliminary investigation of the 1:3 complex between **1** and **3** in acetone-d_6, the signals for H_{du} and H_{eu} shifted upfield and eventually disappeared at 0.01M/0.06M (**1**/**4**). Presumably, the perfect 1:3 complex, **1**(**4**)$_3$, was formed at this concentration. The association constant (K_a) between the salt **1** and **4** is higher than that of the model system (**1** and DB24C8) despite the obvious steric effects by the dendron unit of **4**, suggesting the enhanced solubility of the 1:3 complex resulting from the dendron units overrides the steric penalty at the complexation sites. The signals for the benzylic protons of the dendron unit of **4** also showed distinguishable upfield chemical shifts. The signals for H_n, H_t and H_q, initially resonated as three singlets at 5.25, 5.08 and 5.06 ppm, respectively, but shifted as far upfield as 4.93 ppm upon complexation. The upfield chemical shift may be explained in terms of the interaction of the complexed dendron units with neighboring uncomplexed ammonium salt moieties.

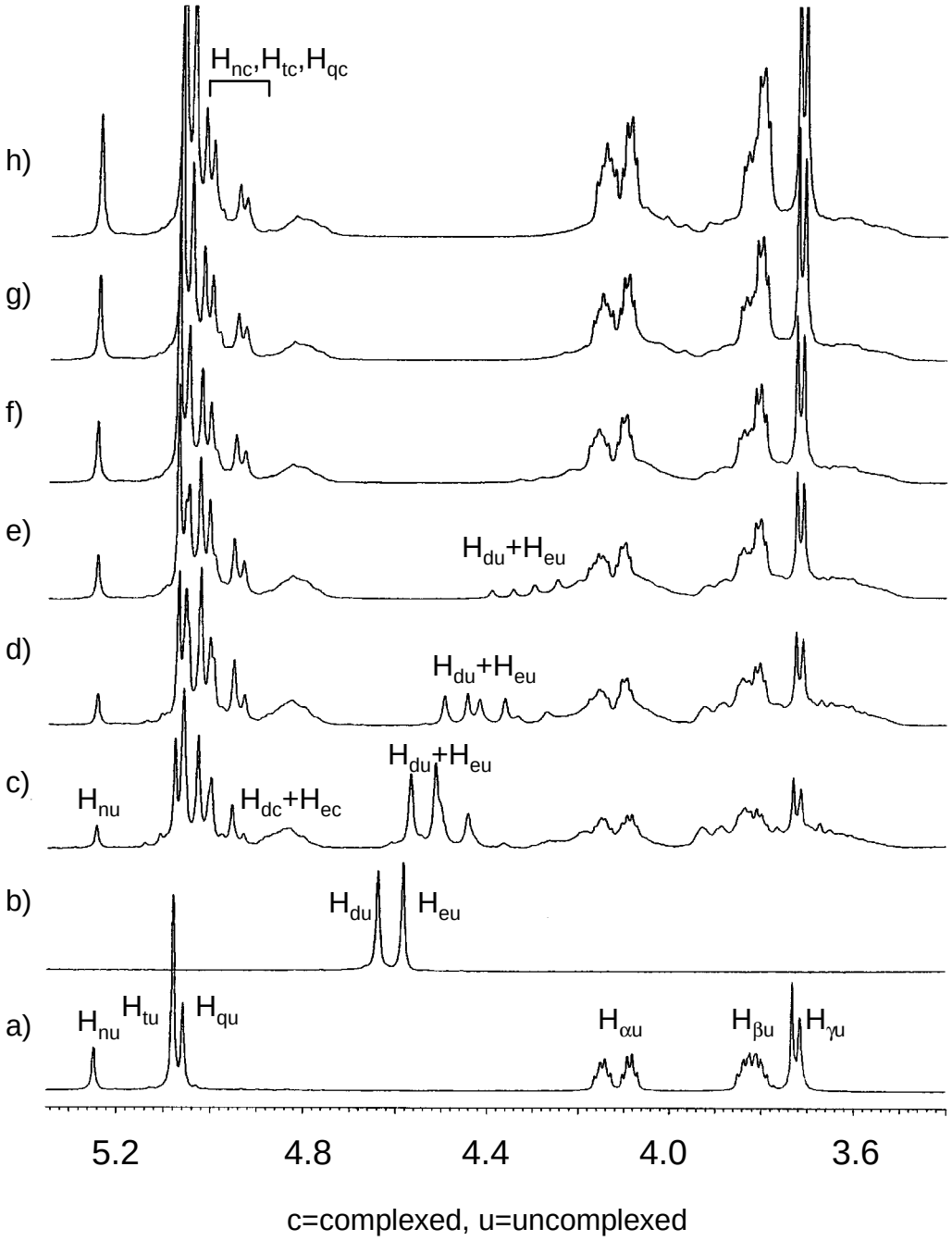

Figure 4.11. The aliphatic region of stacked ^{1}H NMR spectra of solutions of **1** and 2nd generation dendron **4** at a) 0/1.0 x 10^{-2}, b) 1.0 x 10^{-2}/0, c) 1.0 x 10^{-2}/1.0 x 10^{-2}, d) 1.0 x 10^{-2}/2.0 x 10^{-2}, e) 1.0 x 10^{-2}/3.0 x 10^{-2}, f) 1.0 x 10^{-2}/4.0 x 10^{-2}, g) 1.0 x 10^{-2}/5.0 x 10^{-2}, and h) 1.0 x 10^{-2} M/6.0 x 10^{-2} M (400 MHz, acetone-d_6, 22^{o}C).

In the case of the 3rd generation dendritic pseudorotaxane, the ^{1}H NMR spectra of solutions of **1** and **5** in acetone-d_6 (Figure 4.12) exhibit three different sets of signals

(complexed **1** and **5**, free **1** and free **5**) due to slow association and dissociation between the complementary units on the ^{1}H NMR time scale. The signals arising from the benzylic protons of **5**, H_{kc}, H_{nc}, H_{qc}, and H_{tc} (Figure 4.8), exhibit significant upfield chemical shifts upon complexation. This is associated with interactions caused by neighboring dendron units. The signals corresponding to the uncomplexed benzylic protons, H_{du} and H_{eu} (Scheme 3), of the salt **1**, initially located at 4.64 and 4.58 ppm, respectively, drift upfield as **5** is added and eventually fade away with 6 equivalents of **5**. These observations led us to believe that there are no unoccupied ammonium salt moieties in the 0.01M/0.06M solution of **1** and **5**. The association constant of the 3rd generation dendritic pseudorotaxane (1:3 complex) was estimated (K_a = 3.8 x 10^7 M^{-3}) to be 1.8 times higher than that of the model system (1:3 complex from **1** and DB24C8) in acetone despite the apparent steric effects from the dendron units on neighboring complexation sites. We attribute this phenomenon to the excellent solubility of the 1:3 dendritic pseudorotaxane, thus shifting the equilibrium forward.

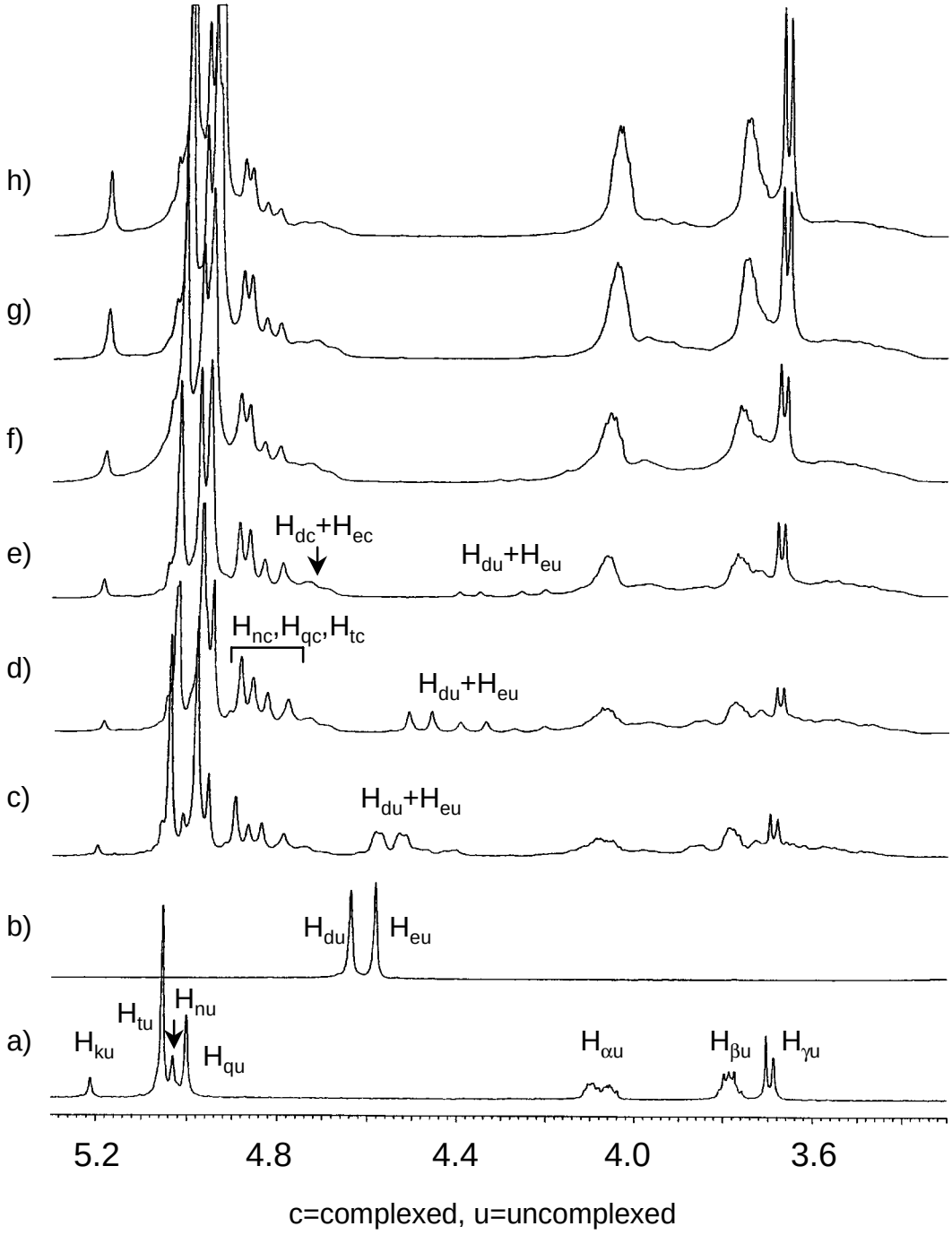

Figure 4.12. The aliphatic region of stacked ^{1}H NMR spectra of solutions of **1** and 3rd generation dendron **5** at a) 0/1.0 x 10^{-2}, b) 1.0 x 10^{-2}/0, c) 1.0 x 10^{-2}/1.0 x 10^{-2}, d) 1.0 x 10^{-2}/2.0 x 10^{-2}, e) 1.0 x 10^{-2}/3.0 x 10^{-2}, f) 1.0 x 10^{-2}/4.0 x 10^{-2}, g) 1.0 x 10^{-2}/5.0 x 10^{-2}, and h) 1.0 x 10^{-2} M/6.0 x 10^{-2} M (400 MHz, acetone-d_6, 22^{o}C).

4.2.3. Mass spectrometry

Gel permeation chromatography (GPC) is routinely used for analyzing dendrimers but it has been demonstrated that accurate molecular weight determination is difficult even with the principle of the universal calibration due to the low hydrodynamic volume of dendrimers.[12] In the present case in chloroform at 25°C **1**(**5**)$_3$ apparently dissociates in the column; only **5** elutes and salt **1** is retained in the column.

Mass spectrometry has been utilized increasingly in the characterization of dendrimers through the use of FAB,[23] ESI,[24] and MALDI-TOF.[25,26] By these analytical methods mass accuracies are in the range of 0.0027-0.10%. The application of these techniques was thus extended to the self-organized dendritic pseudorotaxanes. The 1st and 2nd generation dendrimers were analyzed by FAB mass spectroscopy using different matrices. The FAB mass spectrum recorded for the 1st generation dendritic pseudorotaxane using 3,5-dihydroxybenzoic acid matrix from acetone solvent gave a peak at *m*/*z*=3339.5 for the totally complexed self-assembled dendrimer **1**(**3**)$_3$ after a loss of PF_6^- counter ion (Figure 4.13). The peaks attributed to **1**(**3**)$_2$ and **1**(**3**) after a successive losses of PF_6 units were also detected at *m*/*z*=2400.2 and 1459.2, respectively.

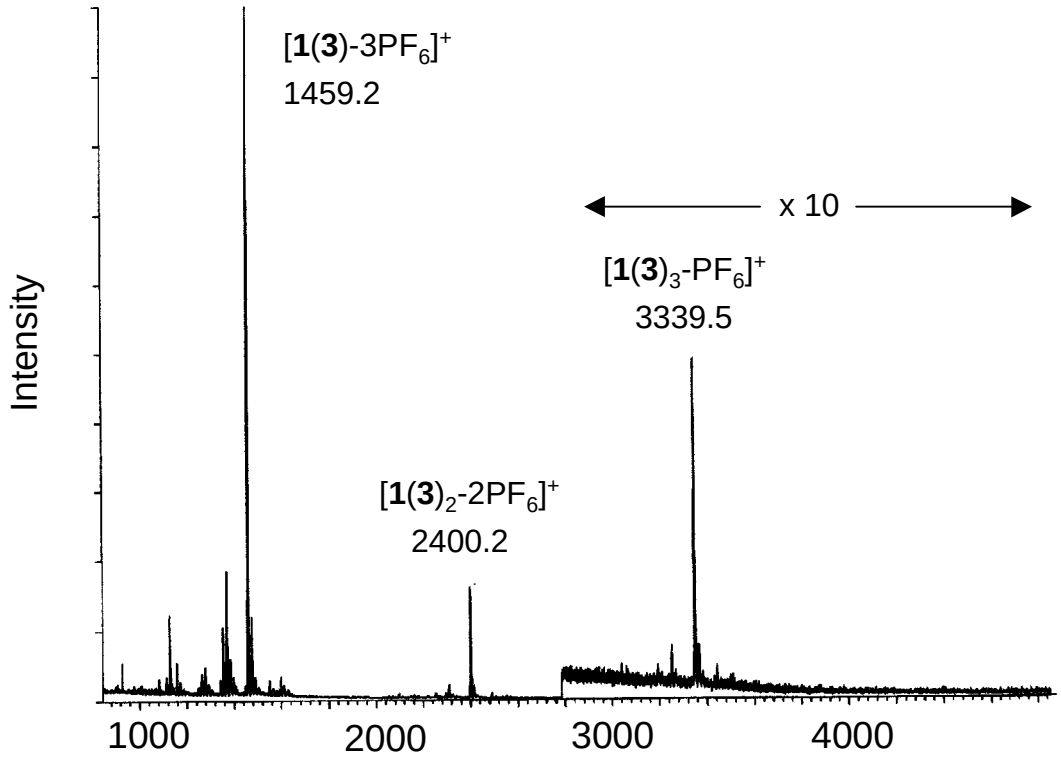

Figure 4.13. The FAB mass spectrum of the 1st generation dendrimer **1**(**3**)$_3$.

Similarly, the FAB mass spectrum for the 2nd generation dendrimer **1**(**4**)$_3$ using trans-3-indoleacrylic acid matrix form THF solvent shows a peak for the perfect dendrimer at *m*/*z*=4611.1 (Figure 4.14). **1**(**4**)$_2$ and **1**(**4**) after losses of two PF_6 units were observed at m/z=3248.7 and 1884.9, respectively. The peaks at m/z=3318.4 and 1954.9 were attributed to [**1**(**4**)$_2$-3PF_6+2HPO_4+Na]$^+$ and [**1**(**4**)-3PF_6+2HPO_4+Na]$^+$, respectively. The formation of HPO_4^{2-}, a hydrolysis product of PF_6^- ion, has been documented.[27]

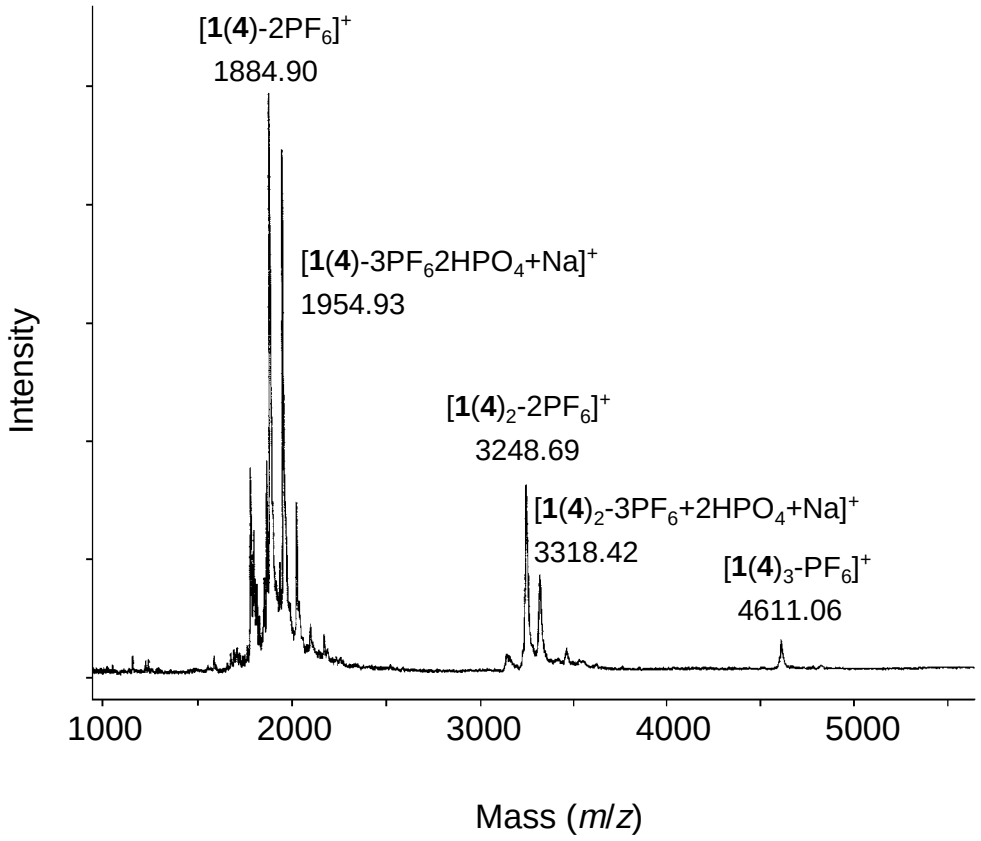

Figure 4.14. The FAB mass spectrum of the 2nd generation dendrimer **1**(**4**)$_3$.

The 3rd generation dendritic pseudorotaxane **1**(**5**)$_3$ was characterized by MALDI-TOF because of its high mass. A 3.0 x 10^{-2} M chloroform solution of **5** was mixed with 1/3 molar equivalent of solid **1** for 3 days. The mixture was then filtered and the filtrate was concentrated to afford a white solid, which was submitted for the MALDI analysis. The spectrum (Figure 4.15) was dominated by three peaks, which correspond to 1:3, 1:2 and 1:1 complexes. The wholly complexed dendritic pseudorotaxane, **1**(**5**)$_3$, was detected at *m/z*=7156.62 after loss of PF_6^-. The 1:2 and 1:1 complexes give rise to the peaks at *m/z*=4945.03 and 2734.18, respectively. The lower abundance side peaks at *m/z*=4854.03 and 2643.2 are found at regular intervals from [**1**(**5**)$_2$-2PF$_6$]$^+$ and [**1**(**5**)-2PF$_6$]$^+$ ($\Delta m/z$ = 91.00 and 90.98, respectively), indicating loss of benzyl groups from the periphery of the dendrons. The apparent distribution of the complexes indicates partial dissociation of **1**(**5**)$_3$ into subunits, **1**(**5**)$_2$ and **1**(**5**), during ionization. It is also noteworthy that MALDI

detectors are nonlinear with respect to molecular mass and thus do not give molar response. ESIMS has to date given similar results; we are currently investigating the use of low sample cone voltage (V_e) to minimize fragmentation. The calculated and observed masses (<0.1% error) of the self-organized dendritic pseudorotaxanes **1**(**3**)$_3$, **1**(**4**)$_3$, and **1**(**5**)$_3$ are summarized in Table 4.1.

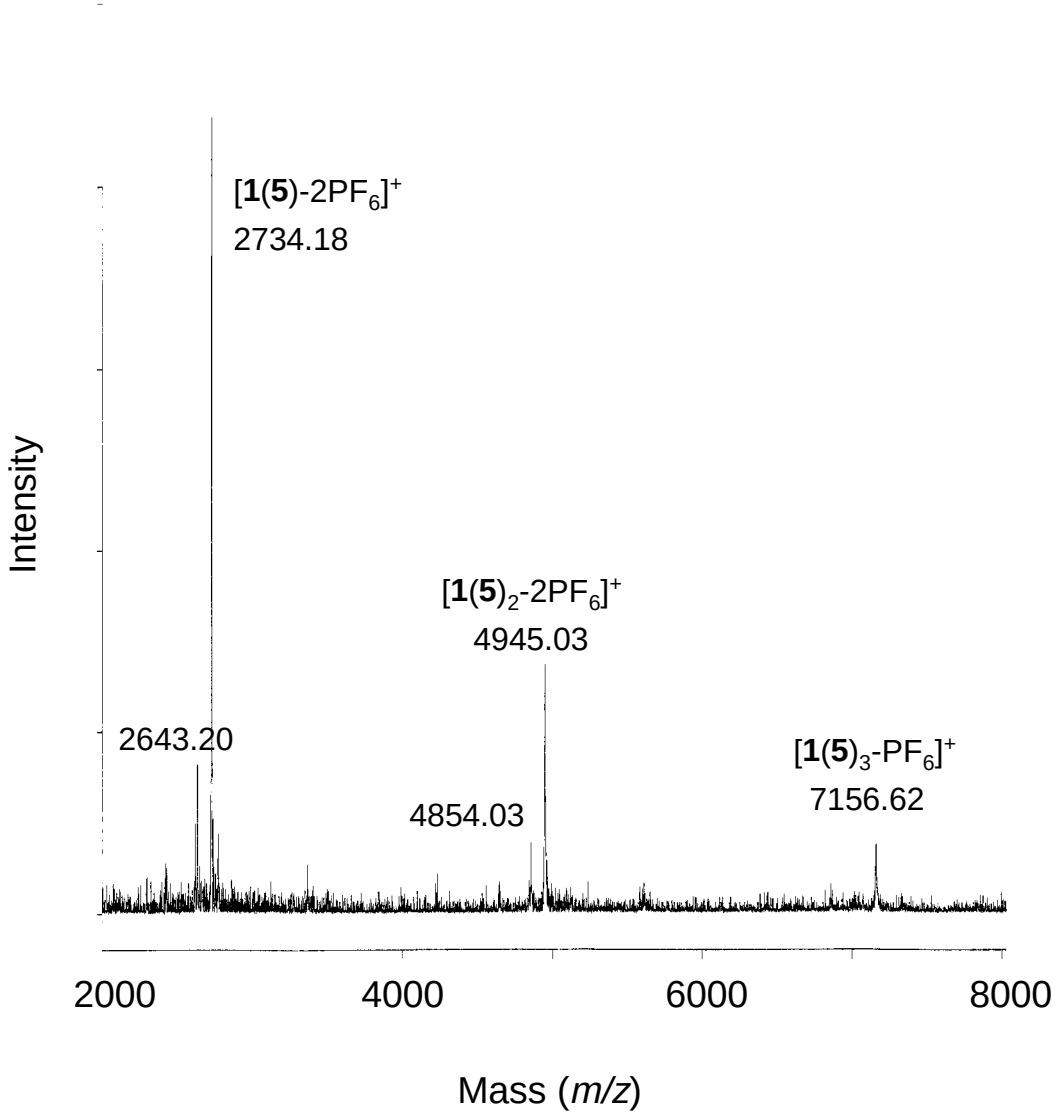

Figure 4.15. The MALDI-TOF mass spectrum of the 3rd generation dendrimer **1**(**5**)$_3$.

Table 4.1. The supramolecular structures, their molecular formulae, calculated molecular weights and observed (ms) mass/charge ratios

structure	molecular formula	calcd MW	obs *m/z*
1(**3**)$_3$-PF$_6$[a]	$C_{48}H_{48}N_3P_2F_{12}(C_{46}H_{50}O_{12})_3$	3339.3	3339.5
1(**3**)$_2$-2PF$_6$[a]	$C_{48}H_{48}N_3PF_6(C_{46}H_{50}O_{12})_2$	2400.0	2400.2
1(**3**)-3PF$_6$[a]	$C_{48}H_{48}N_3(C_{46}H_{50}O_{12})$	1460.7	1459.2
1(**4**)$_3$-PF$_6$[b]	$C_{48}H_{48}N_3P_2F_{12}(C_{74}H_{74}O_{16})_3$	4611.81	4611.06
1(**4**)$_2$-2PF$_6$[b]	$C_{48}H_{48}N_3PF_6(C_{74}H_{74}O_{16})_2$	3248.34	3248.69
1(**4**)-2PF$_6$[b]	$C_{48}H_{48}N_3PF_6(C_{74}H_{74}O_{16})$	1884.88	1884.90
1(**5**)$_3$-PF$_6$[c]	$C_{48}H_{48}N_3P_2F_{12}(C_{130}H_{122}O_{24})_3$	7156.81	7156.62
1(**5**)$_2$-2PF$_6$[c]	$C_{48}H_{48}N_3PF_6(C_{130}H_{122}O_{24})_2$	4945.01	4945.03
1(**5**)-2PF$_6$[c]	$C_{48}H_{48}N_3PF_6(C_{130}H_{122}O_{24})$	2733.22	2734.18

a) The FAB mass spectrum of the 1st generation dendritic pseudorotaxanes was recorded in the positive ion mode using 3-NBA (3-Nitrobenzyl alcohol) as the matrix and acetone as the solvent.
b) The FAB mass spectrum of the 2nd generation dendritic pseudorotaxanes was measured in the positive ion mode with IAA (*trans*-3-Indoleacrylic acid) matrix in THF solvent.
c) The MALDI-TOF spectrum of the 3rd generation dendritic pseudorotaxanes was recorded in the positive ion mode using 2,5-dihydroxybenzoic acid as the matrix and acetone as the solvent.

4.3. Conclusion

In conclusion, we have demonstrated a concise design and efficient construction of various generations of self-organizing pseudorotaxane dendrimers. The ^{1}H NMR investigations in chloroform-*d* indicated self-assembly of the dendritic pseudorotaxanes as a result of a simple recognition between the secondary ammonium salt moieties in **1** and dibenzo-24-crown-8 units at the focal points of the dendron units. Mass spectrometry was also used to characterize the dendritic pseudorotaxanes. The *Chem 3D* molecular modeling of **1**(**3**)$_3$, **1**(**4**)$_3$, **1**(**5**)$_3$ showed disk-shaped aggregates. Figure 4.16 shows the minimized structure of **1**(**5**)$_3$. This self-organizing approach offers the possibility of generating even larger and more complex supramolecular dendrimers.

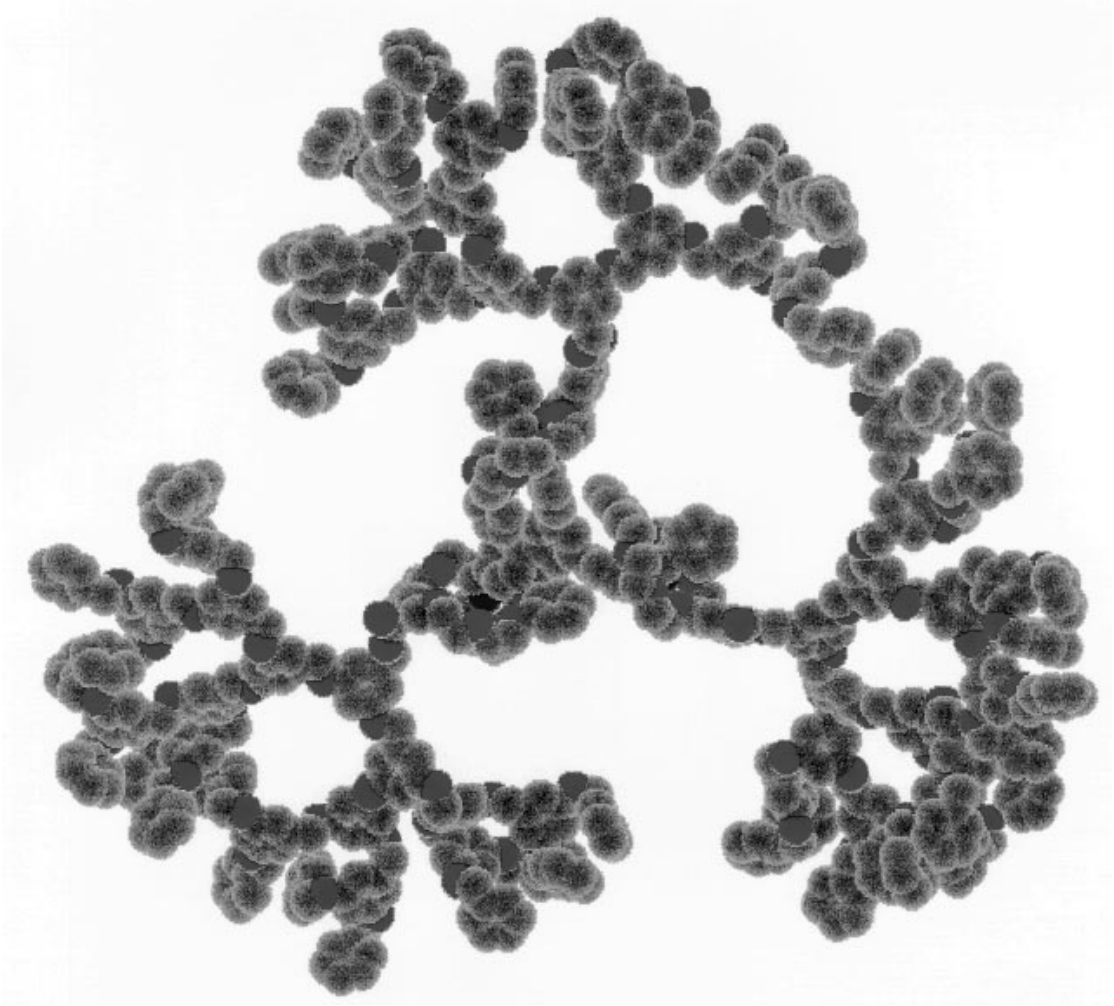

Figure 4.16. The molecular modeling of the 3rd generation dendrimer. The hydrogen atoms are omitted for clarity.

4.4. Experimental

Tetrahydrofuran (THF) was distilled from Na and benzophenone. Pyridine and hexanes were stirred with CaH_2 overnight and distilled. All other solvents were used as received. The 400 MHz ^1H NMR spectra were recorded on a Varian Unity with tetramethylsilane (TMS) as an internal standard. The IR spectra were taken on a Nicolet Impact 400 infrared spectrometer using pulverized KBr as the medium. Gel permeation chromatography (GPC) was performed with an ISCO model 2300, coupled with an ISCO UV detector, using PLgel 5 mm MIXED-D (300 x 7.5 mm) columns and chloroform as solvent and calibrated with PS standards. Molecular modeling was performed on a Dell 200 computer using *Chem3D Pro*™ by Cambridge Scientific Computing, Inc. The

dendritic pseudorotaxanes were first drawn in *ChemDraw Pro*™ and pasted onto *Chem3D Pro*™. The structure was then minimized using MM2 parameters until the root mean square (RMS) gradient was below 0.05. Elemental analyses were obtained from Atlantic Microlab, Norcross, GA. Mass spectra were provided by the Washington University Mass Spectrometry Resource, an NIH Research Resource (Grant No. P41RR0954).

4-Carbomethoxydibenzo-24-crown-8: To a 5 L three necked round bottom flask equipped with a mechanical stirrer, N_2 inlet and a thermometer were added DMF (3.5 L), *n*Bu_4NI (100 mg) and K_2CO_3 (80.60 g, 584 mmol) and the mixture was brought to 110°C. To this were added a solution of *o*-bis(8-chloro-3,6-dioxaoctyloxy)benzene[28] (25.4 g, 61.8 mmol) and methyl 3,4-dihydroxybenzoate (10.4 g, 61.8 mmol) in DMF (120 mL) *via* syringe pump at the rate of 0.75 mL/h. After the completion of the addition, the reaction mixture was vigorously stirred for 3 days, cooled to 25°C, and filtered with the aid of Celite. The solvent was rotary evaporated to give a brown viscous liquid. This was preabsorbed onto silica gel and the product was continuously extracted with Et_2O using a Soxhlet extraction apparatus. After the solvent was removed the resulting yellow solid was recrystallized from EtOH to give a white powder (12.5 g, 40% yield), mp 83-85°C. ^{1}H NMR (400 MHz, chloroform-*d*, 22°C): δ=3.84 (8H, m), 3.87 (3H, s), 3.93 (8H, m), 4.15 (4H, t, *J* = 8.0 Hz), 4.19 (4H, t, *J* = 8.0 Hz), 6.84 (1H, d, *J* = 8.4 Hz), 6.88 (4H, m), 7.52 (1H, d, *J* = 2.0 Hz), and 7.64(1H, dd, *J* = 2.0 and 8.4 Hz); LRFAB: *m/z* = 506.2 $[M]^+$, 475.2 $[M\text{-}OCH_3]^+$; HRFAB: calcd for $[M]^+$ $C_{26}H_{34}O_{10}$ 506.2152, found 506.2132; Anal. Calcd for $C_{26}H_{34}O_{10}$: C, 61.65; H, 6.77, found: C, 61.75; H, 6.80.

4-Carboxydibenzo-24-crown-8: To a 250 mL one-necked round bottom flask were added 4-carbomethoxydibenzo-24-crown-8 (3.16 g, 6.24 mmol) and 100 mL of EtOH. To this was added aq. KOH (4M, 10 mL) dropwise and the reaction mixture was refluxed for 12 h. Upon completion of the reaction the solvent was rotary evaporated to give an off-white solid which was redissolved in H_2O (100 mL) and neutralized with H_2SO_4. The solution was extracted with CH_2Cl_2 (100 mL x 2) and the organic layers were combined,

dried over $MgSO_4$ and concentrated to give a white solid which was recrystallized from EtOH to give a white solid (2.73 g, 89% yield), mp 182-183°C. ^{1}H NMR (400 MHz, chloroform-*d*, 22°C): δ=3.84 (8H, m), 3.93 (8H, m), 4.15 (4H, t, *J* = 4.0 Hz), 4.20 (4H, t, 4.0 Hz), 6.88 (5H, m), 7.56 (1H, d, *J* = 1.6 Hz), and 7.71 (1H, dd, *J* = 1.6 and 8.4 Hz); LRFAB: *m/z* = 531.1 $[M+K]^+$, 492.2 $[M]^+$; HRFAB: calcd for $[M]^+$ $C_{25}H_{32}O_{10}$ 492.1995, found 492.1985; Anal. Calcd for $C_{25}H_{32}O_{10}$: C, 60.97; H, 6.55, found: C, 61.19; H, 6.60.

General procedure for 2, 3 and 4: To a 25 mL round bottom flask equipped with a magnetic stirrer were added the appropriate dendritic benzyl alcohol synthesized in our laboratories ([G1]-OH, [G2]-OH or [G3]-OH) (1.00 equiv.), 4-carboxydibenzo-24-crown-8 (1.00 equiv.), TPP (1.50 equiv.) and THF. To this was added DEAD (1.50 equiv.) dropwise via syringe and the reaction mixture was stirred at 25°C for 10 h. The solvent was evaporated to give a white solid (a yellow viscous liquid in the cases of **3** and **4**) which was subjected to a short column of silica gel using EtOAc as the eluent. The resulting white solid (colorless viscous liquid in the cases of **3** and **4**) was redissolved in EtOAc and precipitated into MeOH to afford a white solid (a clear glass in the cases of **3** and **4**).

[G1]-DB24C8 (2): 84% yield, mp 113-114°C (MeOH). ^{1}H NMR (400 MHz, chloroform-*d*, 22°C): δ=3.84 (8H, m), 3.93 (8H, m), 4.15 (4H, m), 4.20 (4H, m), 5.04 (4H, s), 5.26 (2H, s), 6.59 (1H, t, *J* = 2.0 Hz), 6.67 (2H, d, *J* = 2.0 Hz), 6.84 (1H, d, *J* = 8.8 Hz), 6.88 (4H, m), 7.30-7.43 (10H, m), 7.55 (1H, d, *J* = 2.0 Hz), and 7.67 (1H, dd, *J* = 2.0 and 8.8 Hz); LRFAB: *m/z* = 794.4 $[M]^+$; HRFAB: calcd for $[M]^+$ $C_{46}H_{50}O_{12}$ 794.3302, found 794.3300. Anal. Calcd for $C_{46}H_{50}O_{10}$: C, 69.51; H, 6.34, found: C, 69.43; H, 6.31.

[G2]-DB24C8 (3): 89% yield, colorless glass. ^{1}H NMR (400 MHz, chloroform-*d*, 22°C): δ=3.82 (8H, m), 3.91 (8H, m), 4.13-4.18 (8H, m), 4.97 (4H, s), 5.02 (8H, s), 5.25 (2H, s), 6.55 (1H, t, *J* = 2.0 Hz), 6.56 (2H, t, *J* = 2.0 Hz), 6.65 (2H, d, *J* = 2.0 Hz), 6.67 (4H, d, *J* = 2.0 Hz), 6.81 (1H, d, *J* = 8.4 Hz), 6.84-6.90 (4H, m), 7.31-7.41 (20H, m), 7.54 (1H, d, *J* = 2.0 Hz), and 7.65 (1H, dd, *J* = 2.0 and 8.4 Hz); LRFAB: *m/z* = 1218.6 $[M]^+$; HRFAB: calcd for $[M]^+$ $C_{74}H_{74}O_{16}$ 1218.4977, found 1218.4943. Anal. Calcd for $C_{74}H_{74}O_{16}$: C, 72.89; H, 6.12, found: C, 72.82; H, 6.10.

[G3]-DB24C8 (4): 93% yield, colorless glass. ^{1}H NMR (400 MHz, chloroform-*d*, 22^{o}C): δ=3.81 (m, 8H), 3.89 (m, 8H), 4.13 (m, 8H), 4.95 (s, 12H), 5.01 (s, 16H), 5.23 (s, 2H), 6.53 (t, 2H, *J* = 2.4 Hz), 6.56 (t, 4H, *J* = 2.4 Hz), 6.58 (t, 1H, *J* = 2.4 Hz), 6.66 (m, 14H), 6.80 (d, 1H, *J* = 8.4 Hz), 6.87 (m, 4H), 7.28-7.41 (m, 40H), 7.54 (s, 1H), and 7.64 (d, 2H, *J* = 8.4 Hz); LRFAB: *m/z* = 2090.9 $[M+Na]^+$; HRFAB: calcd for $[M+Na]^+$ $C_{130}H_{122}O_{24}Na$ 2090.8257, found 2090.8227.

4.5. References

1)Sadamoto, R.; Tomioka, N.; Aida, T. *J. Am. Chem. Soc.* **1996**, *118*, 3978-3979.

2)Miller, L. L.; Duan, R. G.; Tully, D. C.; Tomalia, D. A. *J. Am. Chem. Soc.* **1997**, *119*, 1005-1020.

3)van Hest, J. C. M.; Delnoye, D. A. P.; Baars, M. W. P. L.; Elissen-Román, C.; van Genderen, M. H. P.; Meijer, E. W. *Chem. Eur. J.* **1996**, *2*, 1616-1626.

4)Newkome, G. R.; Moorefield, C. N.; Vögtle, F. *Dendritic Molecules: Concepts, Synthesis, Perspectives*; VCH: Weinheim, 1996.

5)Kopelman, R.; Shortreed, M.; Shi, Z.-Y.; Tan, W.; Xu, Z.; Moore, J. S.; Bar-Haim, A.; Klafter, J. *Phys. Rev. Lett.* **1997**, *78*, 1239-1242.

6)Kawa, M.; Fréchet, J. M. J. *Chem. Mater.* **1998**, *10*, 286-296.

7)Jansen, J. F. G. A.; de Brabander-van den Berg, E. M. M.; Meijer, E. W. *Science* **1994**, *266*, 1226-1229.

8)Jansen, J. F. G. A.; Peerlings, H. W. I.; de Brabander-Van den Berg, E. M. M.; Meijer, E. W. *Angew. Chem. Int. Ed. Engl.* **1995**, *34*, 1206-1209.

9)Jansen, J. F. G. A.; Janssen, R. A. J.; de Brabander-Van den Berg, E. M. M.; Meijer, E. W. *Adv. Mater.* **1995**, *7*, 561-564.

10)Jansen, J. F. G. A.; Meijer, E. W. *J. Am. Chem. Soc.* **1995**, *117*, 4417-4418.

11)Moore, J. S. *Acc. Chem. Res.* **1997**, *30*, 402-413.

12)Wooley, K. L.; Hawker, C. J.; Fréchet, J. M. J. *J. Am. Chem. Soc.* **1991**, *113*, 4252-4261.

13)Newkome, G. R.; Yao, Z.; Baker, G. R.; Gupta, V. K.; Russo, P. S.; Sanders, M. J. *J. Am. Chem. Soc.* **1986**, *108*, 849-850.

14)Tomalia, D. A.; Baker, H.; Dewald, J.; Hall, M.; Kallos, G.; Martin, S.; Roeck, J.; Ryder, J.; Smith, P. *Macromolecules* **1986**, *19*, 2466-2468.

15)Kawaguchi, T.; Walker, K. L.; Wilkins, C. L.; Moore, J. S. *J. Am. Chem. Soc.* **1995**, *117*, 2159-2165.

16)Zimmerman, S. C.; Zeng, F.; Reichert, D. E. C.; Kolotuchin, S. V. *Science* **1996**, *271*, 1095-1098.

17)Zeng, F.; Zimmerman, S. C. *Chem. Rev.* **1997**, *97*, 1681-1712.

18)Ashton, P. R.; Collins, A. N.; Fyfe, M. C. T.; Glink, P. T.; Menzer, S.; Stoddart, J. F.; Williams, D. J. *Angew. Chem. Int. Ed. Engl.* **1997**, *36*, 59-62.

19)Ashton, P. R.; Campbell, P. J.; Chrystal, E. J. T.; Glink, P. T.; Menzer, S.; Philp, D.; Spencer, N.; Stoddart, J. F.; Tasker, P. A.; Williams, D. J. *Angew. Chem. Int. Ed. Engl.* **1995**, *34*, 1865-1869.

20)Ashton, P. R.; Chrystal, E. J. T.; Glink, P. T.; Menzer, S.; Schiavo, C.; Spencer, N.; Stoddart, J. F.; Tasker, P. A.; White, A. J. P.; Williams, D. J. *Chem. Eur. J.* **1996**, *2*, 709-728.

21)Mitsunobu, O. *Synthesis* **1981**, *1*, 1-28.

22)Hughes, D. L. *Org. Prep. Proced. Int.* **1996**, *28*, 127-164.

23)Twyman, L. J.; Beezer, A. E.; Mitchell, J. C. *J. Chem. Soc. Perkin Trans.* **1994**, *4*, 407-422.

24)Hummelen, J. C.; van Dongen, J. L. J.; Meijer, E. W. *Chem. Eur. J.* **1997**, *3*, 1489-1493.

25)Leon, J. W.; Fréchet, J. M. J. *Polym. Bull. Berlin* **1995**, *35*, 449-455.

26)Xu, Z.; Kahr, M.; Walker, K. L.; Wilkins, C. L.; Moore, J. S. *J. Am. Chem. Soc.* **1994**, *116*, 4537-4550.

27)Moucheron, C.; Kirsch-De Mesmaeker, A. *J. Am. Chem. Soc.* **1996**, *118*, 12834-12835.

28)Shinkai, S.; Inuzuka, K.; Miyazaki, O.; Manabe, O. *J. Org. Chem.* **1984**, *49*, 3440-3442.